Desalination and Water Treatment
www.deswater.com
1 (2009) 114–127
1944-3994/1944-3986

Simulation of an autonomous, two-stage solar organic Rankine cycle system for reverse osmosis desalination

G. Kosmadakis*, D. Manolakos, S. Kyritsis, G. Papadakis

Department of Natural Resources and Agricultural Engineering, Agricultural University of Athens, 75 Iera Odos Street, 11855 Athens, Greece
Tel. +30 210 529 4033, Fax: +30 210 529 4023; email: gkosmad@central.ntua.gr

Received 10 July 2007; Accepted 14 August 2008

ABSTRACT

The present work concerns the simulation of an autonomous, two-stage solar organic Rankine cycle (SORC) for RO desalination. Aiming at improving the efficiency of the single-stage low temperature (operation temperature range in the order of 70–80°C) SORC for RO desalination, a high temperature (operation temperature range in the order of 140°C) stage is added. The basic principle of operation is that the heat extracted from the condensation of the high temperature stage (e.g. upper stage), evaporates the refrigerant of the low temperature stage (e.g. lower stage), thus significantly increasing the overall efficiency. In comparison with the low temperature single-stage system, the two-stage system exploits much more efficiently the heat produced by the vacuum tube solar collector array, since a higher operational temperature difference between high and low temperature reservoirs is achieved. Moreover, an analysis of the desalination unit takes place so that to estimate the annual desalinated water. The system design was implemented based on TRNSYS V16.0 and ROSA software.

Keywords: Evacuated solar collectors; Solar organic Rankine cycle; RO desalination

1. Introduction

The present work concerns the simulation of an autonomous, two-stage solar organic Rankine cycle for RO desalination. The concept is considered as a research step ahead to the existing experience [1,2] gathered within the framework of project COOP-CT2003-507997. Aiming at improving the performance of the already developed system, with a simultaneous reduction of product water cost of the single-stage system, a high temperature (operation temperature range in the order of 140°C) stage is added and studied theoretically in the current paper. The main goal of the current simulation is to estimate the efficiency and the energy available (MWh) for desalination in order to evaluate the improvement of performance arising from the use of a second SORC stage. According to the theoretical thermodynamic background (i.e. cycle operation in a higher temperature increases the efficiency), there should be an increase in the efficiency and in the specific work, but these results are the expected ones and they might differ from the simulation results [3–6].

In this work the annual simulation of the operation of the SORC–RO will be presented. The investigated system consists of two Rankine cycle stages, the high-temperature stage using R245fa as the working fluid and the low-temperature stage using R134a. A vacuum tube solar collector field supplies heat to the Rankine cycles and the mechanical work produced drives the pumps of the system, including the high-pressure pump of the RO desalination unit [7–14].

The design of the system was based on the results derived from the dedicated simulation work. To achieve

*Corresponding author.

this, TRNSYS V16 simulation software was applied to elaborate the energy and mass balance and simulate the dynamic phenomenon, while ROSA v. 6.1.3 (Reverse Osmosis System Analysis, developed by Dow Chemical Company) was used for the design of the RO desalination unit. For the solar collectors array 54 vacuum tube solar collectors (Solamax 300, Thermomax) were used, representing the heat generator of the actual prototype system.

2. Materials and methods

2.1. Description of the system

The simplified block diagram of Fig. 1 illustrates the basic concept of the system. The process can be briefly described as follows: heat produced by the solar collectors is transformed to mechanical energy through the high temperature solar organic Rankine cycle (HTSORC), the so-called "upper stage", operating at a temperature range of 130 to 140°C. The refrigerant R-245fa was selected for this cycle due to its appropriate thermodynamic properties (critical point, T = 154.05°C, P = 36.4 bar) in the defined temperature range and because it is environmentally friendly [15–21]. The mechanical energy produced in the upper stage drives the high pressure pump (HPP) of the RO unit, representing the only consumption served by this stage itself. During condensation, exchanging of heat to the "lower stage" takes place, thus initiating the low temperature solar organic Rankine cycle (LTSORC) process. In other words, the condenser of the upper stage acts as the evaporator of the lower stage. The HFC-134a is the refrigerant selected as the heat carrier of the LTORC. The mechanical energy generated through the LTORC drives the remaining system consumption including system pump energy demand, except for that of HPP. The final stage of heat exchanging is the preheating of the seawater. There HFC-134a condensates and preheats the seawater from 20°C, so that the efficiency of the RO desalination unit increases.

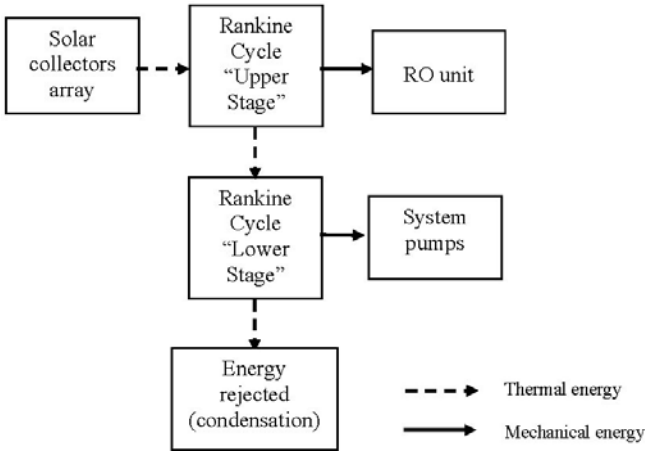

Fig. 1. Simplified block diagram of the system.

The current work focuses on and is based more on quantification of the improvement of the system compared to the single-stage system. Therefore, the selection of the top temperature of the low temperature stage (77°C) was selected so that a straightforward comparison with the single-stage system could be made, and many parameters were kept the same. The top temperature of the high-temperature stage (137°C) was selected so that the supplied solar heat would be the same as in the single-stage system. With this, and keeping the mass flow rate of the organic fluid the same, the evaporation temperature was estimated. It was observed that the efficiency of the collectors and the expander for this temperature is quite satisfactory.

It should be mentioned that according to previous experience, the refrigerant, which will be used for the low-temperature stage, is the HFC-134a. It is not flammable, non-toxic and belongs to the zero-ODP (ozone depletion potential) group of refrigerants. It is widely used and there is a lot of experience with its physical and thermodynamic characteristics [15–21]. The detailed layout of the system under investigation is shown in Fig. 2.

2.2. Simulation of the system

The Rankine thermodynamic cycle is characterized by the following thermodynamic states (Table 1) pointing out their thermodynamic properties (i.e. temperature, pressure, enthalpy, entropy etc.), which are presented in Tables 2a and 2b for HFC-134a; the pressure/enthalpy chart is shown in Fig. 3.

The evaporation temperature is considered at 71.7°C, the superheat temperature before the expansion at 75.8°C, while that after the expansion at 37.81°C. The R134a condensats at 35°C where the heat released supplies the seawater preheater of the RO desalination. The R134a pump increases its pressure and at this stage the working fluid is sub-cooled at 34.22°C and finally it is preheated up to 71.7°C. The heat for both preheating and evaporation is supplied from the condensation process of the high-

Table 1
State changes of the thermodynamic cycle for both stages

1	→	2′:	Isentropic (ideal) expansion
1	→	2:	Non- isentropic (real) expansion
2	→	3:	Isobaric condensation
3	→	4′:	Isentropic (ideal) compression
3	→	4:	Non-isentropic (real) compression
4	→	4′′:	Isobaric preheat
4′′	→	4′′′:	Isobaric evaporation
4′′′	→	1:	Superheat

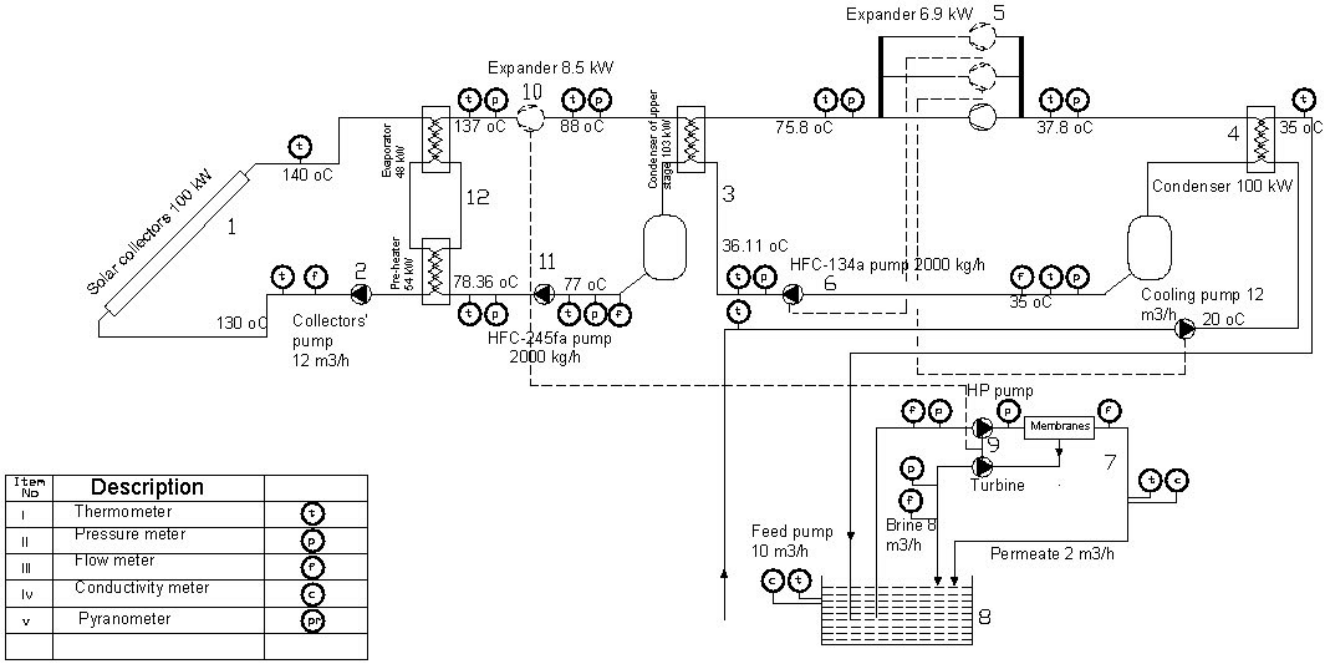

Fig. 2. Layout of the two-stage SORC system.

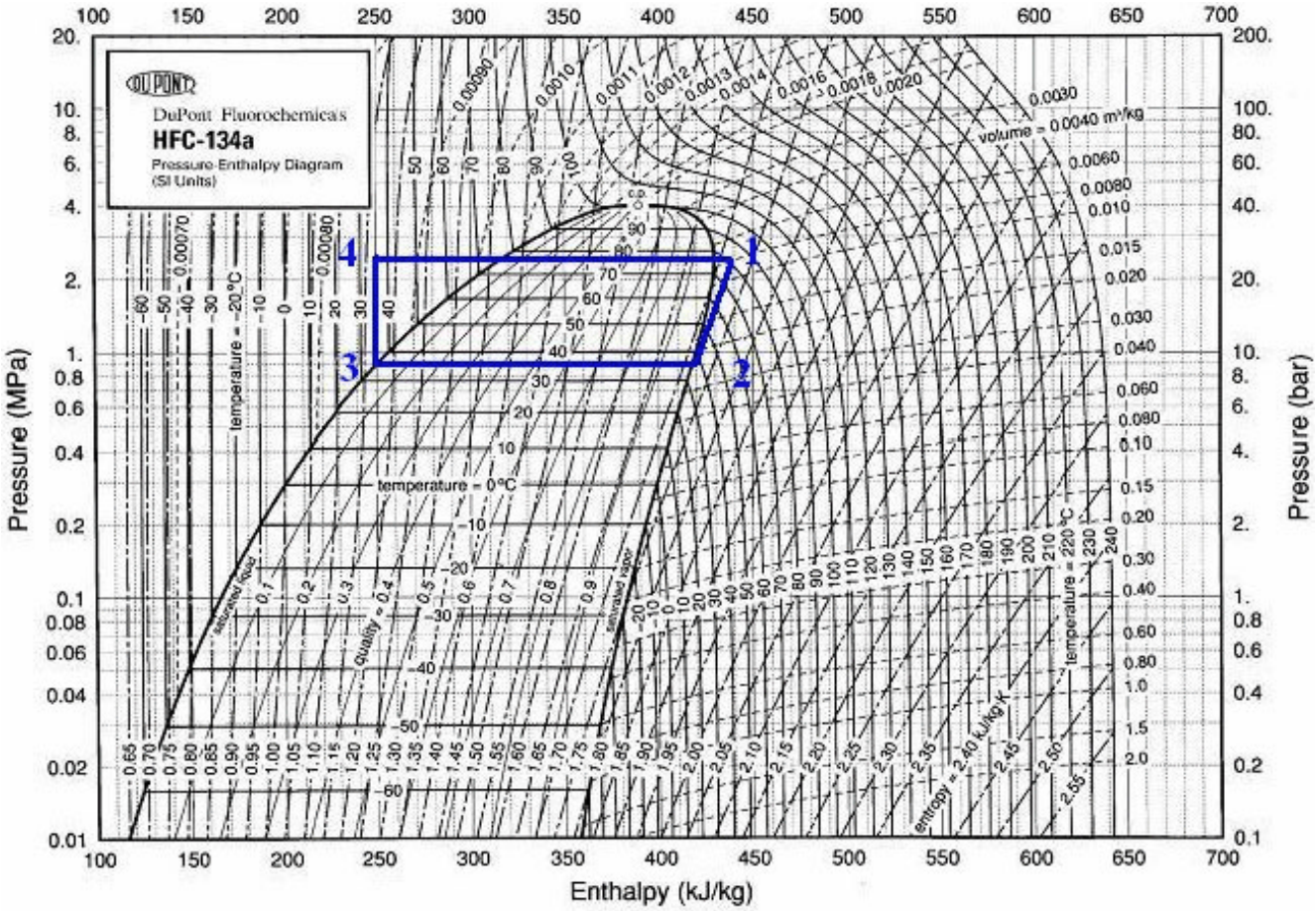

Fig. 3. Pressure/enthalpy chart of Rankine cycle with R134a.

Table 2a
Thermodynamic properties of the low temperature stage

State	Situation	Temp. (°C)	Pressure (bar)	Enthalpy (kJ/kg)
1	Superheated vapor	75.8	22.0	435.70
2′	Saturated vapor (isentropic)	35.00	8.8791	417.50
2	Superheated vapor	37.81	8.8791	420.23
3	Saturated liquid	35.00	8.8791	249.20
4′	Sub-cooled liquid (isentropic)	35.96	22.0	250.33
4	Sub-cooled liquid	36.11	22.0	250.53
4″	Saturated liquid	71.70	22.0	307.80
4‴	Saturated vapor	71.70	22.0	428.84

Table 2b
Thermodynamic properties of the low temperature stage

State	Entropy (kJ/kg/K)	Density (kg/m^3)	Viscosity (Pas)	C_p (kJ/kg/K)
1	1.7138	115.33	1.4757e-05	1.5155
2′	1.7138	43.463	1.2134e-05	1.1031
2	1.7225	42.677	1.2256e-05	1.0866
3	1.1676	1167.30	0.00017192	1.4711
4′	1.1676	1172.92	0.00017480	1.4553
4	1.1682	1172.34	0.00017450	1.4560
4″	1.3433	985.47	0.00010361	1.8374
4‴	1.3433	121.42	1.4662e-05	1.6566

Table 3a
Thermodynamic properties of the high temperature stage

State	Situation	Temp. (°C)	Pressure (bar)	Enthalpy (kJ/kg)
1	Saturated vapor	137.0	26.65	492.53
2′	Superheated vapor (isentropic)	84.70	7.315	470.10
2	Superheated vapor	88.00	7.315	473.46
2″	Saturated vapor	77.00	7.315	461.74
3	Saturated liquid	77.00	7.315	306.03
4′	Sub-cooled liquid (isentropic)	78.15	26.65	307.68
4	Sub-cooled liquid	78.36	26.65	307.97
4″	Saturated liquid	137.0	26.65	405.74

Table 3b
Thermodynamic properties of the high temperature stage

State	Entropy (kJ/kg/K)	Density (kg/m^3)	Viscosity (Pas)	C_p (kJ/kg/K)
1	1.8079	185.8	1.7502e-05	2.08770
2′	1.8079	39.02	1.2443e-05	1.09830
2	1.8180	38.12	1.2584e-05	1.09594
2″	1.7840	40.32	1.2139e-05	1.10610
3	1.3393	1181.0	0.0002176	1.48720
4′	1.3393	1189.9	0.0002249	1.46854
4	1.3402	1189.1	0.0002243	1.46911
4″	1.5963	888.60	9.3687e-05	2.21750

temperature stage. It can be seen that there are only two pressure levels, the low (8.8791 bar) and the high (22 bar) one and any pressure losses in the circuit and in the heat exchangers have been ignored.

For HFC-245fa respectively, Tables 3a and 3b incorporate the thermodynamic values of the various states, and Fig. 4 shows the pressure/enthalpy chart.

In Table 3 it can be seen that the evaporation temperature is 137°C, and the refrigerant is saturated vapor just before the expansion. The condensation temperature is 77°C, where the heat released supplies the low-temperature preheater and evaporator. The R245fa pump increases the pressure (high pressure, 26.65 bar) and subcools the refrigerant at 78.36°C, which is finally preheated up to 137°C (saturated liquid).

It should be mentioned at this point that the design of the two cycles (low-temperature and high-temperature) is differentiated by one critical point. In the first case, there is superheated vapor at the turbine inlet, whereas the second one denotes saturation. This is related to the shape of the thermodynamic cycle of the R245fa, where the slope ds/dT of the saturated vapor line is approximately zero or slightly negative. This means that, as mentioned before, R245fa is characterized as isentropic (or slightly dry) while R134a as isentropic refrigerant [22].

In the following section the behavior of the organic Rankine cycle throughout the year is analyzed. In order to do that, the meteorological data of the site of Hellenikon in Athens are used, incorporated in TRNSYS V16 (legally licensed to the Agricultural University of Athens). The meteorological data of the Marathon site (area near Athens, Greece, where the facility has been recently installed) were not available, so the data of Hellenikon have been used without serious error due to the proximity of both areas. The data used are hourly values of the following parameters: ambient temperature, solar zenith and solar azimuth angle, total radiation on the tilted surface and horizontal and sky diffuse radiation on tilted and horizontal surfaces. The data reader and the radiation processor in TRNSYS V16 are incorporated in type109.

All the above data are inserted to an evacuated tube collector component (type 71, TRNSYS V16) and its efficiency, according to the average temperature (inlet-outlet temperature), is computed. At this point it is possible to compute the heat supplied by the solar collectors to the high temperature stage and start the first trials, according to previous experience, for the various flow

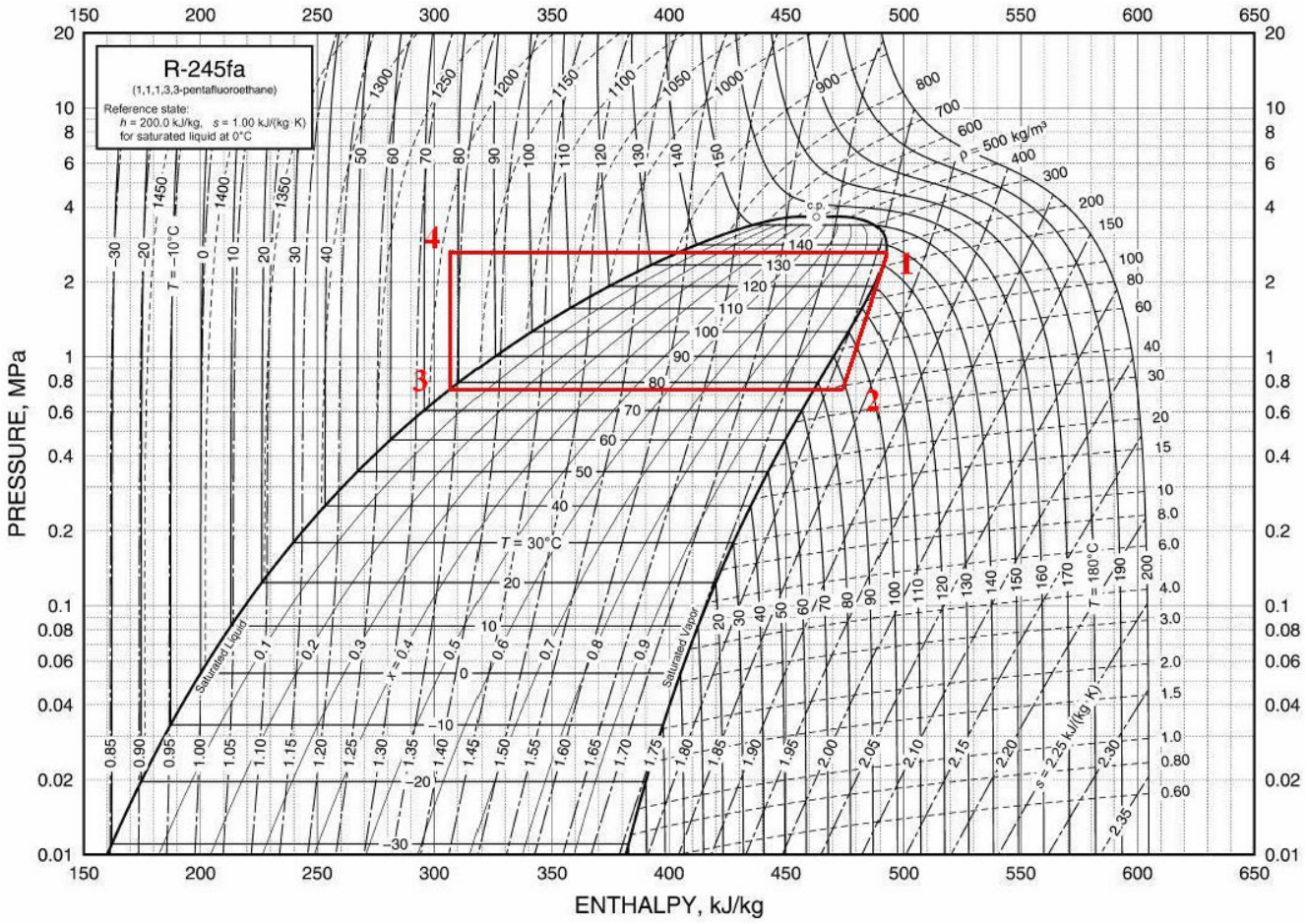

Fig. 4. Pressure/enthalpy chart of Rankine cycle with R245fa.

rates. The optical efficiency is equal to 0.0769 for the specific collector, the linear heat loss factor equal to 1.61 Km^2/W and the square heat loss factor equal to 0.0032 K^2m^2/W. It should be mentioned that the collector's efficiency is given by the following equation:

$$n = n_0 - a_1 \cdot \frac{\Delta T}{G} - a_2 \cdot \frac{\Delta T^2}{G} \quad (1)$$

Fig. 5 presents the collector's efficiency as a function of heating temperatures. It can be seen that for high temperatures, representing the case study, the efficiency is in the order of 33%, a high enough value, taking into consideration the energy gain from the evaporation of R245fa at the considerably high temperature of 137°C. On the horizontal axis there is the temperature difference of the water at the collector outlet and the ambient (the latter is considered constant and equal to 20°C).

The circuit of the collector consists of the solar collectors, the collector pump and the hot side of the high-temperature preheater and evaporator. The hot side

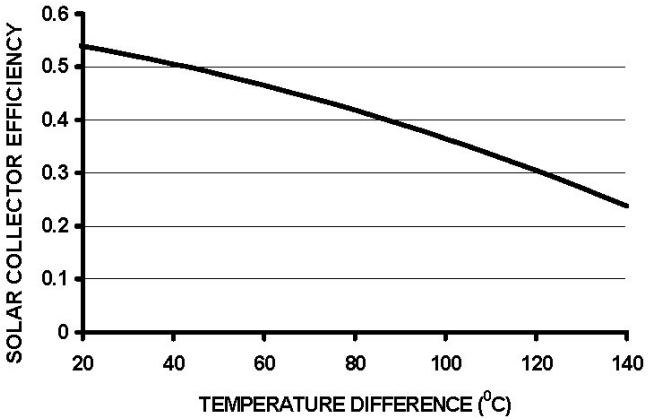

Fig. 5. Efficiency of the solar collector as a function of different outlet temperatures.

(source) working fluid circulating in both heat exchangers is tap water, while that of cold side (load) is the refrigerant R245fa. After being evaporated, R245fa is expanded, producing mechanical work. The condensation processing follows the expansion, providing the condensation heat to

the preheater and evaporator of the R134a circuit (low temperature stage). After evaporating, it is expanded and produces the mechanical work and finally it condensates, while the condensation heat preheats the seawater. The total mechanical work produced must be enough to balance the pump consumption and to supply the RO desalination unit with energy as well.

A preliminary study was conducted in order to have a first estimation for the flow rates of the pumps set. Considering that heat is exchanged between stages and that the thermodynamic cycles should not be altered, the following conclusions were extracted [6,23–27]. The heat produced from the collectors is actually used for preheat and evaporation of the high-temperature stage. The actual collector flow rate of the prototype installation was 3.33 kg/s (12,000 kg/h). This value was also adopted in this analysis, thus defining the pump power to 10,800 kJ/h or 3 kW. Based on this, a first estimation for the flow rate of the R245fa pump can be made. The heat produced by the solar collector field is given by the equation below:

$$Q_{collector} = \dot{m}_{collector} c_p \left(T_{coll,out} - T_{coll,in)}\right) = Q_{preheater,1} + Q_{evaporator,1} = \dot{m}_{R245\,fa}\left(H_{evap1,out} - H_{preh1,in}\right) \quad (2)$$

It is concluded that the flow rate of R245fa is 0.555 kg/s (2000 kg/h) approximately. Table 3 indicates that the enthalpy difference of the R245fa of compression is 1.94 kJ/kg. This value multiplied by the flow rate gives a first estimation of the pump power, which is in the range of 3880 kJ/hr (1.077 kW).

Since the condensation heat of the high-temperature stage is actually the heat supply for the low-temperature stage, the following equation incorporates the energy balance of heat exchanging between the two stages:

$$Q_{cond,1} = Q_{preheater,1} + Q_{evaporator,1} - Q_{T1} = Q_{preheater,2} + Q_{evaporator,2} = \dot{m}_{R134a}\left(H_{evap2,out} - H_{preh2,in}\right) \quad (3)$$

The R134a flow rate is also approximately 0.555 kg/s (2000 kg/h). From Table 2 it can be seen that the enthalpy difference of R134a before and after compression is 1.33 kJ/kg. This value multiplied by the flow rate gives us a first estimation of the pump power, which is in the range of 2660 kJ/h (0.74 kW).

The preheating of seawater is supplied by heat, which is calculated by the formula below:

$$Q_{preheater,2} + Q_{evaporator,2} - Q_{T2} = \dot{m}_{seawater} c_p \left(T_{seawater,out} - T_{seawater,in}\right) \quad (4)$$

The seawater flow rate is around 1.388 kg/s (5000 kg/h), while the pump power is approximately 10,800 kJ/h (3 kW). The same pump as that of the collector circuit is chosen. It should be mentioned that the collector pump flow rate is constant, when there is sufficient power and the flow rate of the rest pumps is variable, so that the thermodynamic cycles of the organic working fluids to be kept constant.

In TRNSYS V16, pump operation is simulated by the type 3b component. The collector pump, as well as the R245fa pump, the R134a pump and the seawater preheat pump use this TRNSYS type. The maximum mass flow rate is 12,000 kg/h for the collector pump (constant), 2000 kg/h for the R245fa pump (variable), 2000 kg/h for the R134a pump (variable) and 5000 kg/h for the seawater pump (constant).

The preheater and evaporator of the high-temperature stage, as well as those of the low-temperature stage, cannot be simulated by any TRNSYS V16 component, so external equations were formed. The equations that are being used are the following.

- Heat provided from the solar collectors:

$$Q_{collector} = \dot{m}_{collector} c_p \left(T_{coll,out} - T_{coll,in}\right) \quad (5)$$

- Enthalpy of water at different locations (collectors, seawater circuit):

$$H_w = c_p T_w \quad (6)$$

- Evaporation specific heat:

$$Q_{evaporator} = H_{evap,out} - H_{evap,in} \quad (7)$$

- Specific preheat:

$$Q_{preheat} = H_{pr,out} - H_{pr,in} \quad (8)$$

- Isentropic efficiency:

$$n_{is,T} = \frac{H_{T,out} - H_{T,in}}{H_{T,out,is} - H_{T,in}} \quad (9)$$

There is an enthalpy difference between the real and the ideal point after the expansion. There has been some interpolation, linear or exponential, according to which method best feeds the data. The resulting equations are of the form:

$$\Delta H_{T,is} = f\left(H_{T,in}\right) \quad (10)$$

- Mechanical power produced by the turbine:

$$W_T = \dot{m}_T \left(H_{T,out} - H_{T,in} \right) \quad (11)$$

- Condensation specific heat:

$$Q_{condensation} = H_{cond,out} - H_{cond,in} \quad (12)$$

- Heat supplied to the low-temperature stage:

$$Q_{low} = Q_{collector} - Q_{T1} \quad (13)$$

- Heat supplied for the preheating of seawater:

$$Q_{seawater} = Q_{collector} - W_{T1} - W_{T2} \quad (14)$$

It is of importance to mention that, in case the heat produced from the collectors decrease, the mechanical work produced from the turbines decreases as well. This means that the power supplied to all pumps also decreases because this is actually a specific portion of the whole power production. According to the characteristic curve of operation, a change in the pump power results not only in a change in the flow rate, but in the outlet pressure as well. The dependence of the flow rate from the pump power is stronger and more straightforward and it is assumed that when power changes only the flow rate changes, so that the thermodynamic proper-ties of the two cycles (high-temperature and low-temperature cycles) remain unchanged.

3. Results and discussion of the simulation

3.1. Simulation of the solar organic Rankine cycle

The results of the simulation are presented and analysed. Yearly simulation time interval (8760 h) and hourly time-steps have been considered. The relaxation factor used in TRNSYS V16 is 0.1. The results concern:

- annual mechanical work production
- flow rate of the pumps set
- energy consumed by the pumps
- net available energy (the difference of the energy produced and the energy consumed at the pumps)
- heat exchanged between water and R245fa (high-temperature stage), R245fa and R134a (low-temperature stage) and R134a and seawater (seawater preheat)
- efficiency of the two-stage organic Rankine cycle

The results are presented for two representative days corresponding to extreme climatic conditions in terms of solar radiation intensity and temperature, which are the 21st of January and the 21st of July. Some cumulative results of the calculated quantities are also presented.

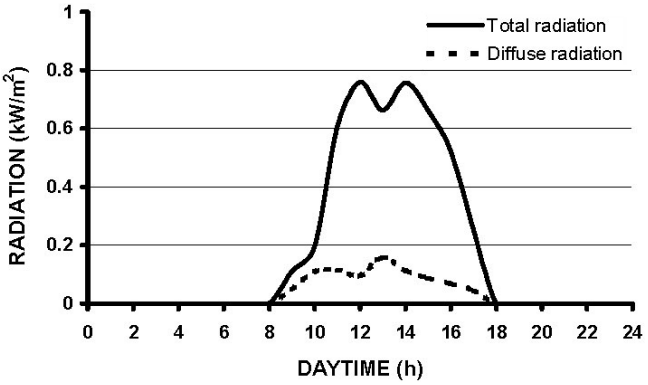

Fig. 6. Total radiation and diffuse radiation on tilted surface during the winter day.

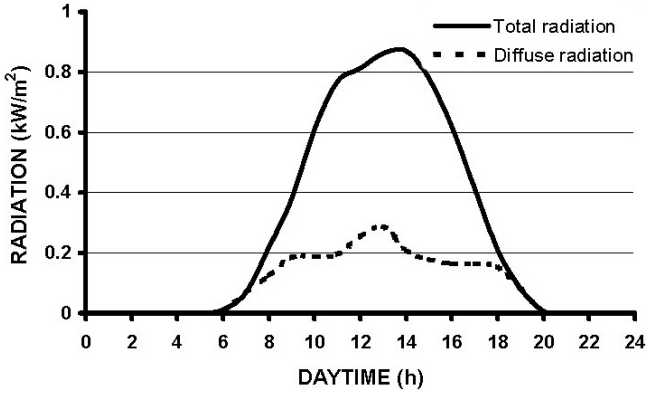

Fig. 7. Total radiation and diffuse radiation on tilted surface during the summer day.

The analysis begins with the radiation on the tilted surface (40° slope of surface). The total and diffuse radiation for the winter and for the summer day are presented in Figs. 6 and 7. The values of the radiation for the summer are higher, especially for the diffuse radiation. It should be mentioned that the form of the slope of the radiation is familiar with all the figures to be presented next, since radiation is the first and most important factor that influences all the calculated values, for example the mechanical power produced. This is the reason that all the following slopes will have a quite same form as the radiation for each season.

Figs. 8 and 9 present the mechanical work produced by the two turbines during a winter and summer day respectively. The mechanical efficiency of the turbines was set constant and equal to 0.85. The expander is a scroll type expander, which is a critical component making the system more efficient and cost effective. Its efficiency is much higher compared to conventional expanders, since it has been taken from automobile air-conditioning systems and its rotation speed can be 8000 RPM or

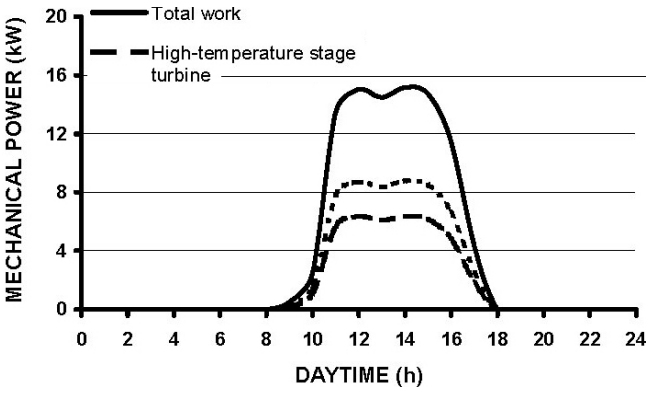

Fig. 8. Mechanical work of the high-temperature stage turbine, of the low-temperature stage turbine and of the total mechanical work during the winter day.

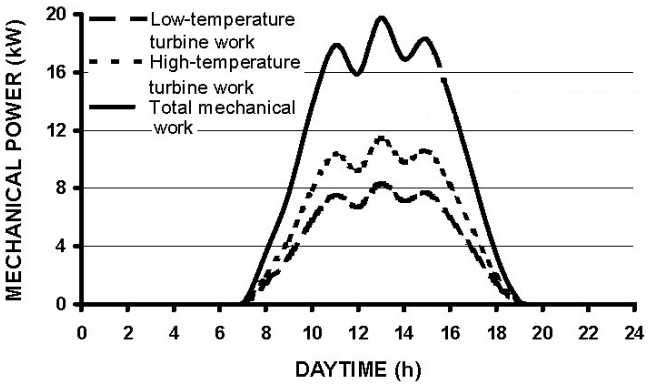

Fig. 9. Mechanical work of the high-temperature stage turbine, of the low-temperature stage turbine and of the total mechanical work during the summer day.

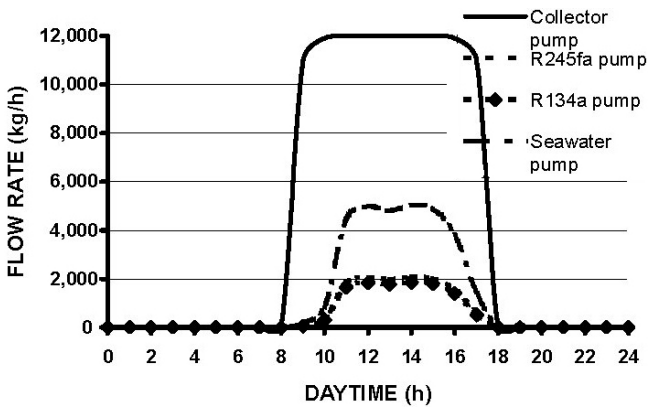

Fig. 10. Flow rate of the collector pump of the R245fa, of the R134a and of the seawater for the winter day.

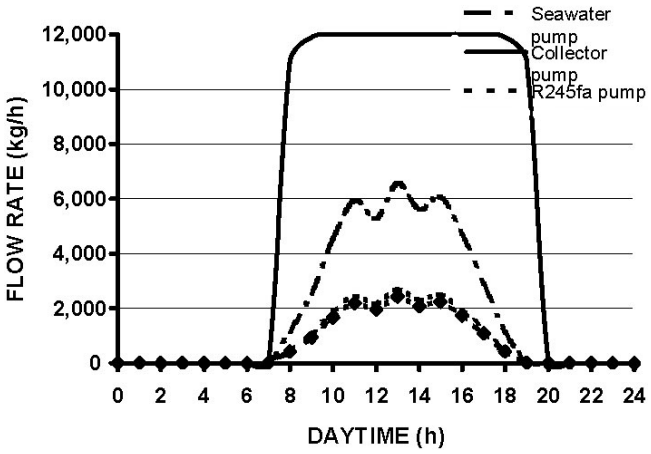

Fig. 11. Flow rate of the collector pump, of the R245fa, of the R134a and of the seawater for the summer day.

more. Actually is a scroll type compressor in reverse operation that in normal operation efficiency of more than 90% is expected. It can be observed that the first expander produces more power since it operates at a higher temperature range.

The same conclusions can be extracted here. The first turbine produces more power again and the difference between the total mechanical work in the summer and in the winter can be clearly observed. Also during the summer, the daytime is longer thus more mechanical power is being produced. The production starts at 7 am and finishes at 7 pm during the specific summer day, while during the winter day it starts at 8 am and finishes at 6 pm.

The flow rate of the different pumps is examined next during the summer and winter days studied. The form of the curves is expected to be the same with these of the mechanical work for the summer and winter respectively. The results can be seen in Figs. 10 and 11.

The form of the curves is analogous to the ones of the production of mechanical work. When the organic Rankine system operates, the collector pump flow rate is exactly 12,000 kg/h. The flow rate of the seawater pump is around 5000 kg/h, according to the preliminary design, and the R245fa and R134a pumps have almost the same flow rate and around 2000 kg/h with the first one being slightly higher.

The pump consumption is a linear function of the pump flow rate. It is considered that every pump has a constant coefficient of efficiency equal to 0.75. The direct linkage of pumps is done coaxially (pump-turbine of the energy recovery system) having a pulley in between identical to that of the expander, having a transmission ratio 1:1 and no gear box is applied. In Figs. 12 and 13 the power consumption for every pump, as well as the total pump consumption for the winter day and the summer day, are illustrated.

The mechanical power produced by the two turbines should be more than the power demand of the pumps, so that the net power production (mechanical power–power for the pumps) can drive the high-pressure pump and

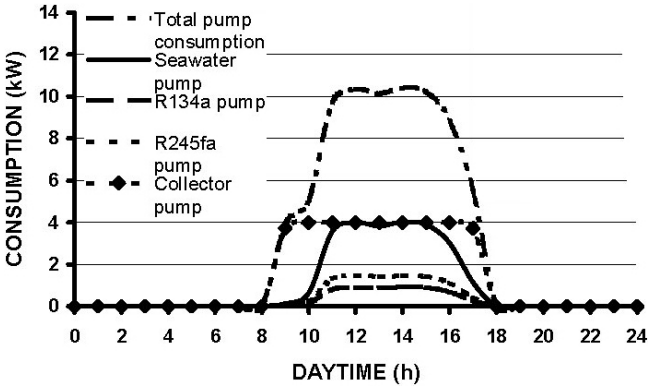

Fig. 12. Consumption of the collector pump of the R245fa of the R134a of the seawater and the total pump consumption on the 21st of January.

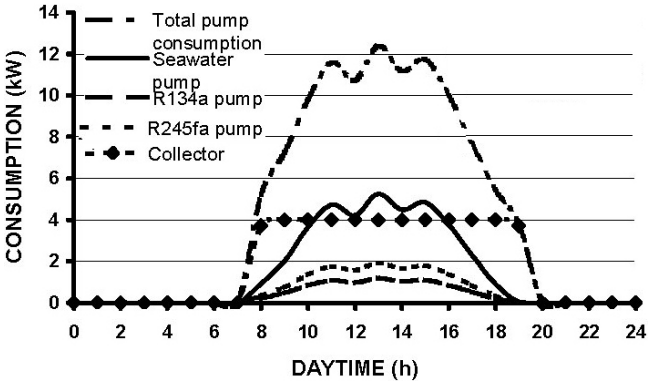

Fig. 13. Consumption of the collector pump, of the R245fa, of the R134a, of the seawater and the total pump consumption on the 21st of July.

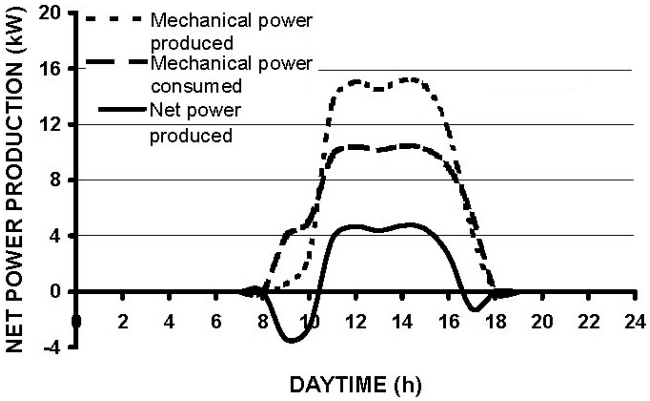

Fig. 14. Net power production of the organic Rankine system mechanical power produced, consumed power for the pumps for the winter day.

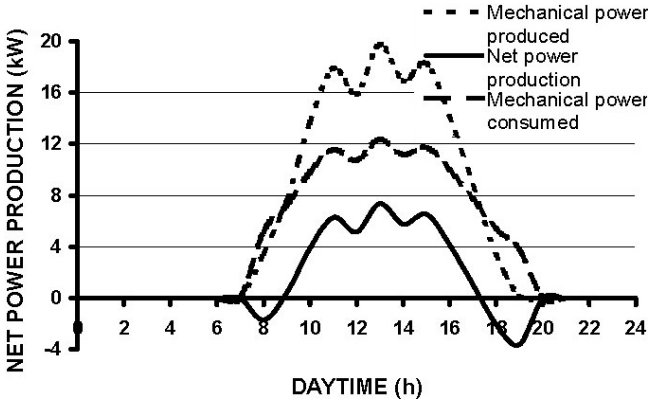

Fig. 15. Net power production of the organic Rankine system, mechanical power produced, consumed power for the pumps for the summer day.

desalinate the seawater in the RO desalination unit. It should be noted that the energy recovery system of the RO unit and the expander are connected directly through the pulley-belt arrangement. When the power produced by the expander is sufficient to initiate the RO process, the RO unit starts to operate. In terms of pressure, at the start point the available pressure takes over the osmotic pressure. This practically means a definite pressure difference of the Rankine cycle. There is not any special control adopted, which is an aspect of a future optimization work to be done in a future project. The system starts and stops according to the available mechanical power incorporating the solar radiation availability. This net energy flow is visualized in Figs. 14 and 15 for the winter day and the summer day respectively.

Early in the morning and late in the afternoon there are some intervals where the produced mechanical power is not sufficient. At these time periods the system does not operate because it cannot cover its own energy needs. For example, on the winter day, the power production begins at 8 am, but the actual system operation starts at around 10 am, the moment when the net energy production becomes positive and ends at around 4.30 pm. In the summer day the power production starts at 9 am and it stops at 5 pm.

Finally, a small proportion of the heat produced from the collectors can be converted by the turbines into mechanical work. A large proportion that preheats the seawater can be seen in Figs. 16 and 17 for winter and summer day respectively.

The efficiency of the organic Rankine system for the winter day is:

$$n_{eff} = \frac{W_{T1} + W_{T2} - \sum W_{PUMPS}}{Q_{collector}} = 0.0381 \quad (15)$$

The efficiency takes a quite large value if it is taken into consideration that during the winter the system starts to operate when the net power production is positive, while the efficiency of the organic Rankine system for the summer day is:

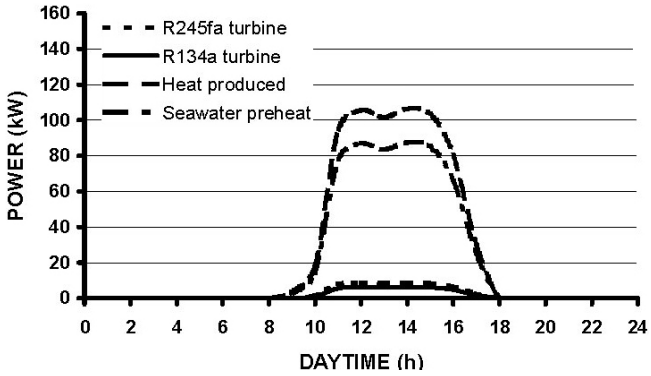

Fig. 16. Heat produced from the collectors, mechanical work produced in the high-temperature stage turbine and in the low-temperature stage turbine and seawater preheat during the winter day.

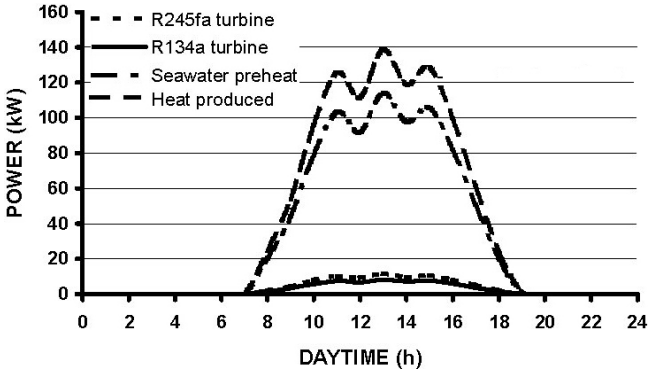

Fig. 17. Heat produced from the collectors, mechanical power produced in the high-temperature stage turbine and in the low-temperature stage turbine and seawater preheat during the summer day.

$$n_{eff} = \frac{W_{T1} + W_{T2} - \sum W_{PUMPS}}{Q_{collector}} = 0.0412 \quad (16)$$

which is slightly higher than the winter efficiency.

To summarize the analysis of the results, the daily and annual energy balance is presented in Table 4. When the net energy production is negative, the values at that time are also taken into consideration, although the system does not be operate then.

The efficiency of the system throughout the year is around 3.2% and the net energy production is approximately 6.7 MWh, which is available exclusively for the desalination of the preheated seawater.

In conclusion, the energy capacity of every component in the two-stage organic Rankine cycle, according to its maximum power can be seen in Table 5. According to the table with the data concerning the time, when the maximum operational intensity of the system takes place, the efficiency for that moment only is 5.145%, which is higher than the one that was calculated before. This is because the desalination unit is actually working at its maximum load. It should be mentioned at this point that in the energy balances the seawater pump consumption is taken into account, but not the benefit from this preheat (if the seawater pump consumption was not taken into consideration, then the efficiency for that case would be

Table 4
Energy results for the winter and summer day and for the whole year

	Winter day	Summer day	Annual
Heat produced from the collectors, kWh	643.89	983.82	208815.42
Energy for the collector pump, kWh	24.00	36.00	7488.00
Energy for the R245fa pump, kWh	8.28	13.10	2418.31
Energy for the R134a pump, kWh	5.09	8.02	1486.68
Energy for the seawater pump, kWh	22.4	35.30	6534.82
Sum of energy of pumps, kWh	59.77	92.42	17927.81
Mechanical energy of turbine 1, kWh	48.80	77.00	14264.35
Mechanical energy of turbine 2, kWh	35.50	56.00	10375.46
Sum of mechanical energy of turbines, kWh	84.30	133.00	24639.81
Net energy production [(sum of turbines)−(sum of pumps)], kWh	24.53	40.58	6712
Coefficient of efficiency, %	3.81	4.125	3.214

Table 5
Maximum power of the different components

Component	Power (kW)
Collectors	138
Collectors pump	4
R245fa pump	2
R134a pump	1.6
Seawater pump	5.2
R245fa turbine	11.8
R134a turbine	8.1
Water/R245fa preheater	74.96
Water/R245fa evaporator	63.04
Water/R245fa total heat exchangers	138
R245fa/R134a preheater	40.384
R245fa/R134a evaporator	85.816
R245fa/R134a total heat exchangers	126.2
R134a/Seawater preheater	118.1

8.913%, which is a quite high value). If a direct comparison is made with the autonomous low-temperature solar Rankine cycle system for a RO desalination unit [1], the efficiency can be calculated with a more general formula:

$$n_{eff} = \frac{W_{T1} + W_{T2}}{Q_{collector}} \quad (17)$$

For the single-stage organic Rankine cycle the efficiency is around 7% [1], whereas for the two-stage cycle it is 11.8%. This means that there is an increase of 68% of the efficiency with the addition of the high-temperature stage, which is a very important improvement.

3.2. Simulation of the reverse osmosis desalination unit

One easy way for calculating the production of the desalinated water is that a cubic meter of seawater demands around 2.5 kWh [1,2]. In the current case for the entire year there are available around 6.7 MWh. This means that 2680 m^3 of seawater can be desalinated every year. A more detailed analysis for the desalination unit is deployed through the ROSA v. 6.1.3 (Reverse Osmosis System Analysis) software by Dow Chemical. With this software all the parameters and characteristics of the reverse osmosis desalination unit will be determined.

The water that is going to be desalinated is seawater. The seawater flow rate is 10 m^3/h, its temperature 35°C and the system's recovery efficiency is 20%. In Table 6 the chemical properties of the seawater can be seen.

The RO desalination unit consists of one stage with three membranes in each vessel. Their type is SW30HR-320, so that a straightforward comparison with the low-temperature organic Rankine cycle can be made. As mentioned before, the recovery is 20%, meaning that the permeate flow is 2 m^3/h and the concentrate flow is 8 m^3/h. In Fig. 18 the system configuration can be seen.

It should be mentioned that according to this analysis the specific energy consumption is 9.75 kWh/m^3, which will be reduced, when energy recovery will be taken into consideration. The properties of the different states of the seawater can be seen in Table 7, according to Fig. 18.

The system details are listed in Table 8. The most important values are those of the power and of the specific energy because the efficiency of the two-stage organic Rankine cycle depends a lot on these values. It should be noted that so far no energy recovery has been involved. This factor will be taken into consideration in the next paragraph.

As was mentioned before, the specific energy consumption without energy recovery is 9.75 kWh/m^3. This means that for the winter day the desalinated water production is around 2.5 m^3, whereas for the summer day it is 4.2 m^3. In Table 9 the water production can be seen for the winter day, for the summer day and for the whole year. These values are computed without taking into account the energy recovery, which will greatly increase the desalinated water production.

The desalinated water flow rate can be seen in Fig. 19 for both the winter and summer days. It is observed that in the summer the flow rate is higher and also as it was

Table 6
Composition of the seawater (type: open intake, SDI <5)

Ions	mg/l	ppm $CaCO_3$	meq/l	Total conc. (mg/l)
Ammonium (NH_4)	0	0	0	0
Potassium (K)	32.011	40.933	0.819	32.01
Sodium (Na)	12850.82	27948.710	558.974	12850.82
Magnesium (Mg)	1506.495	6196.506	123.930	1506.49
Calcium (Ca)	383.126	955.903	19.118	383.13
Strontium (Sr)	0	0	0	0
Barium (Ba)	0	0	0	0
Carbonate (CO_3)	10.934	18.221	0.364	10.93
Bicarbonate (HCO_3)	129.927	106.489	2.130	129.93
Nitrate (NO_3)	0	0	0	0
Chloride (Cl)	20399.95	28770.420	575.408	20399.95
Fluoride (F)	0	0	0	0
Sulfate (SO_4)	5997.047	6246.924	124.939	5997.05
Silica (SiO_2)	0.2	n.a.	n.a.	0.2
Boron (B)	0	n.a.	n.a.	n.a.
Total dissolved solids: 41310.5 mg/l				
Cations: 702.84				
Anions: 702.84				
pH: 7.6				

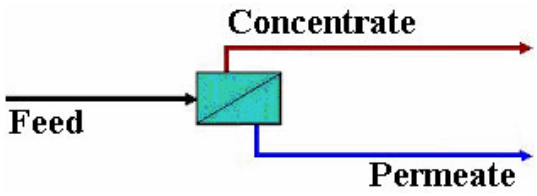

Fig. 18. System configuration of the reverse osmosis unit.

Table 7
Properties of the different states of the seawater

Stream	Flow (m^3/h)	Pressure (bar)	TDS (mg/l)
Feed (before high-pressure pump)	10.00	0.00	41,310.52
Feed (after high-pressure pump)	10.00	56.15	42,709.56
Concentrate	8.00	54.70	53,326.02
Permeate	2.00	—	249.50
	% Recovery	20.00	

Table 8
System details

Feed flow to stage 1, m^3/h	10.00
Raw water flow to system, m^3/h	10.00
Feed pressure, bar	56.15
Fouling factor	0.85
Chemical dose	None
Total active area, m^2	89.18
Water classification	Seawater (open intake) SDI <5
Pass 1 permeate flow, m^3/h	2.00
Pass 1 recovery, %	20.00
Feed temperature, °C	35.0
Feed TDS, mg/l	42,709.56
Number of elements	3
Average pass 1 flux, lmh	22.43
Osmotic feed pressure, bar	31.63
Osmotic concentrate pressure, bar	39.96
Osmotic average pressure, bar	35.79
Average NDP, bar	19.46
Power, kW	19.50
Specific energy, kWh/m^3	9.75

mentioned before, the clean water production lasts for a longer period of time during the day.

In the next paragraph the energy recovery will be taken into consideration and the same tables and charts will be given so that the positive influence of the energy recovery will be revealed. The benefit is an extra power production in a turbine because of the high-pressure of the concentrate (brine) water. The inlet pressure is 54.70 bar and the outlet pressure is the ambient (1 bar). The flow rate of the concentrate water can be calculated according

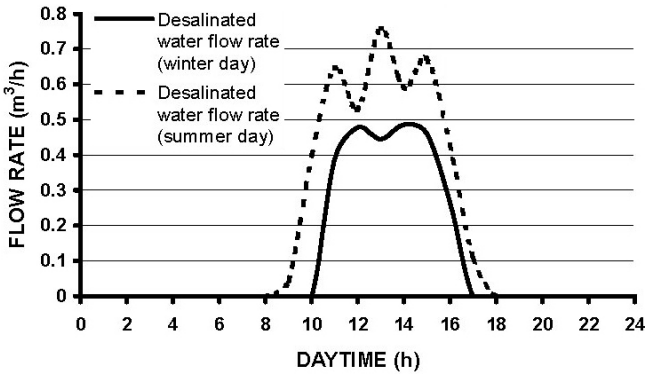

Fig. 19. Desalinated water flow rate during the winter and summer days.

Table 9
Energy properties of the two-stage desalination unit (without energy recovery)

	Winter day	Summer day	Annual
Net energy production (kWh)	24.53	40.58	6712
Specific energy consumption (kWh/m^3)	9.75	9.75	9.75
Power (kW)	19.50	19.50	19.50
Desalinated water (m^3)	2.516	4.162	688.41
Specific thermal energy ($kW_{th}h/m^3$)	255.92	236.38	303.33

Table 10
Energy properties of the two-stage desalination unit (with energy recovery)

	Winter day	Summer day	Annual
Net energy production (without energy recovery), kWh	24.53	40.58	6712
Specific energy consumption (without energy recovery), kWh/m^3	9.75	9.75	9.75
Specific energy consumption (with energy recovery), kWh/m^3	2.5	2.5	2.5
Power (without energy recovery), kW	19.50	19.50	19.50
Power (with energy recovery), kW	19.50	19.50	19.50
Desalinated water (without energy recovery), m^3	2.516	4.162	688.41
Desalinated water (due to energy recovery), m^3	7.296	12.07	1996.39
Total desalinated water (with energy recovery), m^3	9.812	16.232	2684.8
Specific thermal energy (without energy recovery), $kW_{th}h/m^3$	255.92	236.38	303.33
Specific thermal energy (with energy recovery), $kW_{th}h/m^3$	65.62	60.61	77.78

to the water recovery of the desalination unit, which is 20%. The result of the energy recovery is the decrease of the specific energy consumption to around 2.5 kWh/m^3, meaning that more desalinated water is produced. In this point the variables of Table 9 can be computed in the case of the energy recovery. The results are once again for the winter day, for the summer day and for the whole year. It can be observed that the specific energy consumption decreases dramatically because of the energy recovery, and also the desalinated seawater increases almost three times. The above can be seen in Table 10 where the values with and without energy recovery are incorporated.

4. Conclusions

The solar organic Rankine cycle is an alternative thermal desalination technology incorporating the RO desalination process. The two-stage system design presented has the capacity to produce about 2684.8 m^3/y fresh water, when an evacuated tube solar generator of 162 m^2 of absorber area is used. Compared to the single-stage Rankine RO process, the efficiency of the two-stage thermodynamic process is radically increased (efficiency increased from 7% to 11.8%) and also desalinated water production increased around 260% [1]. The process studied constitutes an alternative desalination method competitive to PV RO on the basis of techno-economic feasibility, and it seems that it is worthy of further investigation. Although the simulation runs were made as realistically as possible, the system should be also experimentally exploited, in order to have a more detailed view of its operation characteristics and the measured values of the energy and fresh water produced. This is actually the next step in the research study.

5. Symbols

c_p — Specific heat of the water/seawater, kJ/kg/K
G — Global solar radiation, W/m^2
H_w — Water enthalpy, kJ/kg
$H_{evap1,out}$ — outlet enthalpy of the R245fa from the evaporator, kJ/kg
$H_{evap2,out}$ — Outlet enthalpy of the R134a from the evaporator, kJ/kg
$H_{preh1,in}$ — Inlet enthalpy of the R245fa to the preheater, kJ/kg
$H_{preh2,in}$ — Inlet enthalpy of the R134a to the preheater, kJ/kg
$H_{T,in}$ — Inlet enthalpy of the fluid, kJ/kg
$H_{T,out}$ — Outlet enthalpy of the fluid, kJ/kg
$H_{T,out,is}$ — Outlet enthalpy of the fluid in case of an isentropic expansion, (kJ/kg)
$m_{collector}$ — Flow rate of the collector, kg/s
m_{R134a} — Flow rate of R134a, kg/s
m_{R245fa} — Flow rate of R245fa, kg/s
$m_{seawater}$ — Flow rate of the seawater, kg/s
m_T — Flow rate of the organic fluid in the turbine, kg/s
n — Efficiency
n_0 — Optical efficiency
n_{eff} — Efficiency of the solar organic Rankine system
$n_{is,T}$ — Isentropic efficiency
n_m — Mechanical efficiency of the turbine
$Q_{collector}$ — Collector heat, kW
$Q_{evaporator,1}$ — Water/R245fa evaporator, kW
$Q_{evaporator,2}$ — R245fa/R134a evaporator, kW
Q_{low} — Heat supplied to the low-temperature stage, kW
$Q_{preheater,1}$ — Water/R245fa preheater, kW
$Q_{preheater,2}$ — R245fa/R134a preheater, kW
Q_{T1} — High-temperature stage turbine power, kW
Q_{T2} — Low-temperature stage turbine power, kW
$T_{coll,in}$ — Inlet temperature of the collector, °C
$T_{coll,out}$ — Outlet temperature of the collector, °C
$T_{seawater,out}$ — Outlet temperature of the seawater from the preheater, °C
$T_{seawater,in}$ — Inlet temperature of the seawater from the preheater, °C
T_w — Temperature of the water, °C
W_{PUMPS} — Total power consumption of the pumps except from the RO high-pressure pump, kW
W_T — Mechanical power of the turbine, kW
W_{T1} — Total mechanical power produced during expansion from the first stage, kW
W_{T2} — Total mechanical power produced during expansion from the second stage, kW

Greek

α_1 — Linear heat loss factor, Km^2/W
α_2 — Square heat loss factor, K^{2}m^2/W
$\Delta H_{T,is}$ — Isentropic difference during the expansion, kJ/kg
ΔT — Collector–ambient temperature difference, K

Acknowledgements

This work was conducted within the framework of the projects COOP-CT-2003-507997 (partly financed by the European Commission) and 05NON-EU-219 (partly financed by the General Secretary of Research and Technology).

References

[1] D. Manolakos, G. Papadakis, E.Sh. Mohamed, S. Kyritsis and K. Bouzianas, Design of an autonomous low-temperature solar Rankine cycle system for reverse osmosis desalination. Desalination, 183 (2005) 73–80.

[2] D. Manolakos, G. Papadakis, S. Kyritsis and K. Bouzianas, Experimental evaluation of an autonomous low-temperature solar Rankine cycle system for reverse osmosis desalination. Desalination, 203 (2007) 366–374.

[3] V. Maizza and A. Maizza, Working Fluids in non-steady flows for waste energy recovery systems, Appl. Thermal Eng., 16 (1996) 579–590.

[4] V. Maizza and A. Maizza, Unconventional working fluids in organic Rankine-cycles for waste energy recovery systems. Appl. Thermal Eng., 21 (2001) 381–390.

[5] J.L. Wolpert and S.B. Riffat, Solar-powered Rankine system for domestic applications, Appl. Thermal Eng., 16 (1996) 281–289.

[6] Y. Ying and E.J. Hu, Thermodynamic advantages of using solar energy in the regenerative Rankine power plant, Appl. Thermal Eng., 19 (1999) 1173–1180.

[7] B. Bouchekima, B. Gros, R. Ouahes and M. Diboun, Brackish water desalination with heat recovery. Desalination, 138 (2001) 147–155.

[8] G. Caruso and A. Naviglio, A desalination plant using solar heat as heat supply, not affecting the environment with chemicals. Desalination, 122 (1999) 225–234.

[9] E.E. Delyannis, Status of solar assisted desalination: a review. Desalination, 67 (1987) 3–19.

[10] A.M. El-Nashar, Optimizing the operating parameters of solar desalination plants. Solar Energy, 48 (1992) 207–213.

[11] A.M. El-Nashar, Abu Dhabi solar distillation plant. Desalination, 52 (1985) 217–234.

[12] A.M. El-Nashar, An optimal design of a solar desalination plant. Desalination, 93 (1993) 597–614.

[13] L. Garcia-Rodriguez and C. Gómez -Camacho, Perspectives of solar desalination. Desalination, 136 (2001) 213–218.

[14] W. Luft, Five solar-energy desalination systems. Inter. J. Solar Energy, 1 (1982) 21–32.

[15] C.A. Lommers, Air Conditioning and Refrigeration Industry, Refrigerant Selection Guide, 7th ed., Australian Institute of Refrigeration Air conditioning and Heating Inc (AIRAH) Level 7, Melbourne, 2003.

[16] S. Devottat, S. Gopichand and V. Rao Pendyala, Comparative assessment of some HCFCs, HFCs and HFEs as alternatives to CFCll. Inter. J. Refrig., 17(1) (1994) 32–39.

[17] D.R. Defibaugh and G. Morrison, Interaction coefficients for 15 mixtures of flammable and non-flammable components. Inter. J. Refrig., 18(8) (1995) 518–523.

[18] J.R. Sand, S.K. Fischer and P.A. Joyner, Modeled performance of non-chlorinated substitutes for CFC-11 and CFC-12 in centrifugal chillers, International CFC and Halon Alternatives Conference, 1991.

[19] Montreal Protocol on Substances that Deplete the Ozone Layer, Report of the Refrigeration, Air-Conditioning and Heat Pumps Technical Options Committee, 1998.

[20] S. Devotta and V. Rao Pendyala, Thermodynamic screening of some HFCs and HFEs for high-temperature heat pumps as alternatives to CFCl14. Inter. J. Refrig., 17(5) (1994) 338–342.

[21] J.M. Calm and D.A. Didion, Trade-Offs in Refrigerant Selections: Past, Present and Future, Refrigerants for the 21st Century, ASHRAE/NIST Refrigerants Conference, National Institute of Standards and Technology, 1997.

[22] G. Morrison, The shape of the temperature-entropy saturation boundary. Inter. J. Refrig., 17(7) (1994) 494–504.

[23] A. Borsukiewicz-Gozdur and W. Nowak, Maximizing the working fluid flow as a way of increasing power output of geothermal power plant, Appl. Thermal Eng., 27 (2007) 2074–2078.

[24] D. Wei, X. Lu, Z. Lu and J. Gu, Performance analysis and optimization of organic Rankine cycle (ORC) for waste heat recovery. Energy Conv. Manage., 48(4) (2007) 1113–1119.

[25] G. Angelino and C. Invernizzi, General method for the thermodynamic evaluation of heat pump working fluids. Intern. J. Refrig., 11(1) (1988) 16–25.

[26] T. Yamamoto, T. Furuhata, N. Arai and K. Mori, Design and testing of the Organic Rankine Cycle. Energy, 26 (2001) 239–251.

[27] V.M. Nguyen, P.S. Doherty and S.B. Riffat, Development of a prototype low-temperature Rankine cycle electricity generation system, Appl. Thermal Eng., 21 (2001) 169–181.